Electronic Supplementary Material (ESI) for ChemComm.

Electronic Supplementary Information

Distinction of *trans-cis* photoisomers with comparable optical properties in a multiple-state photochromic system – Examining a molecule with three azobenzenes via *in situ* irradiation NMR

Jonas Kind[1], Lukas Kaltschnee[1], Martin Leyendecker[1] and Christina M. Thiele[1]

[1]Clemens-Schöpf-Institut für Organische Chemie und Biochemie, Technische Universität Darmstadt, Alarich-Weiss-Str. 16, D-64287 Darmstadt, Germany

*E-Mail: cthiele@thielelab.de, Phone: +49 6151 16-21830

Table of Contents:

Index of Figures:

Index of Tables:

ESI-1 Synthesis and purification of the azobenzene-benzene-1,3,5-tricarboxyamide (BTA 1)

The N^1,N^3,N^5-tris(4-(phenyldiazenyl)phenyl)benzene-1,3,5-tricarboxamide BTA **1** (Main text Fig. 1) was prepared from benzenetricarboxychloride and 4-aminoazobenzene according to the literature.[1, 2] The crude product was purified by recrystallisation from a THF/MeOH mixture.
Benzenetricarboxychloride and triethylamine were purchased from Sigma Aldrich and were used as delivered. 4-aminoazobenzene was purchased from Acros Chemicals and used as delivered.

ESI-2 UV/Vis experiments

Low concentration UV/VIS experiments:

UV/Vis absorption spectroscopy was carried out with a Jasco V-630 spectrophotometer. Solutions with different concentrations of the BTA **1** were prepared in DMSO. The stock solution was prepared by dissolving 0.3 mg BTA **1** in 10 mL DMSO. The stock solution was diluted in a volumetric flask with DMSO. Dilute solutions were measured in quartz cuvettes with 1 cm path length.

ESI-Table 1: Concentrations of the BTA **1** solutions used for UV/Vis spectroscopy.

Solution	c [µmol/L]
stock solution	402
1:20	20.5
1:100	4.02

Irradiation of the UV/Vis samples was carried out with the same setup as for *in situ* irradiation NMR (ESI-4). To obtain irradiation time dependent absorption spectra, irradiation with UV light and measurement of UV/Vis spectra were executed in an alternating fashion. During measurement of UV/Vis spectra the silica waveguide was removed from the sample solution.

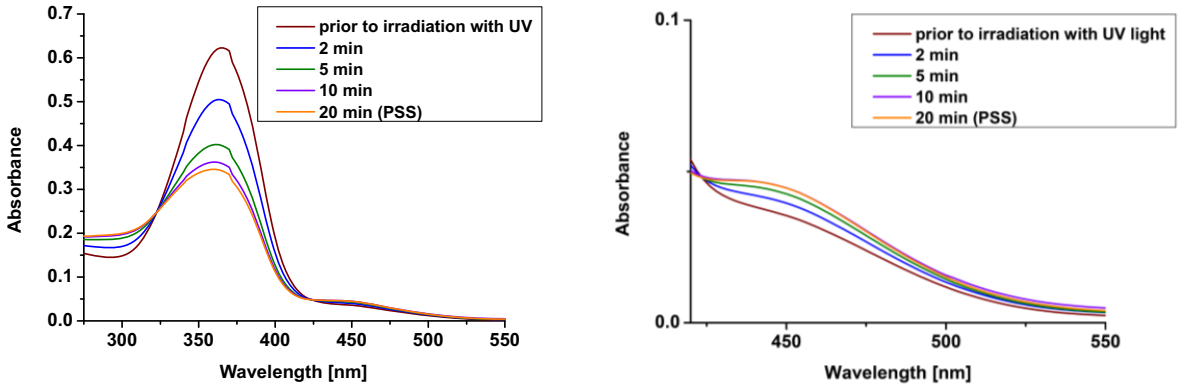

ESI-Figure 1: Left: UV/Vis spectra of a 4 µM solution of BTA **1** prior to and during irradiation with UV light (λ = 365 nm) in DMSO. Right: Magnification of the region between 420 and 550 nm. During irradiation of the sample with UV light an increasing absorbance can be observed in this spectral region.

UV/Vis spectra of the 4 µM BTA solution show a decrease of the absorbance without a shift of the absorption maximum. In contrast, UV/Vis spectra of the 20 µM and 1.8 mM (see high concentration experiment; ESI-Figure 4) BTA solution show a shift of the absorption maximum to a lower wavelength.

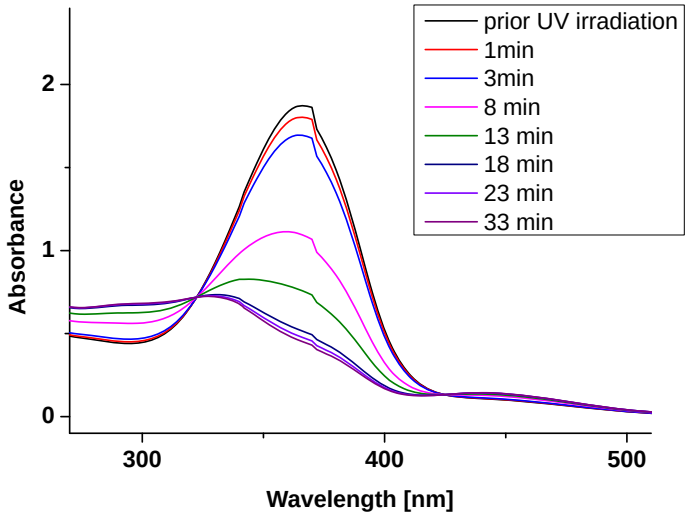

ESI-Figure 2: Absorption spectra of a 20 µM solution of BTA **1** in DMSO at RT prior to irradiation with UV light (black) and after different irradiation times. With increasing irradiation time a decreasing absorbance in the region between 325 nm and 420 nm and an increasing absorbance below 320 nm and above 420 nm is observed. In contrast to the more diluted sample a shift of the absorption wavelength is observed.

In general, for photochromic *trans-cis* isomerization reactions a pseudo zeroth or pseudo first order reaction rate law is expected, depending on irradiation intensity and concentration of the photochromic compound. An irradiation-time dependent absorbance in UV/Vis spectra of the 4 µM BTA solution can be described with monoexponential functions (ESI-Fig. 3), so that a pseudo first order reaction can be assumed for this BTA concentration and irradiation intensity applied.

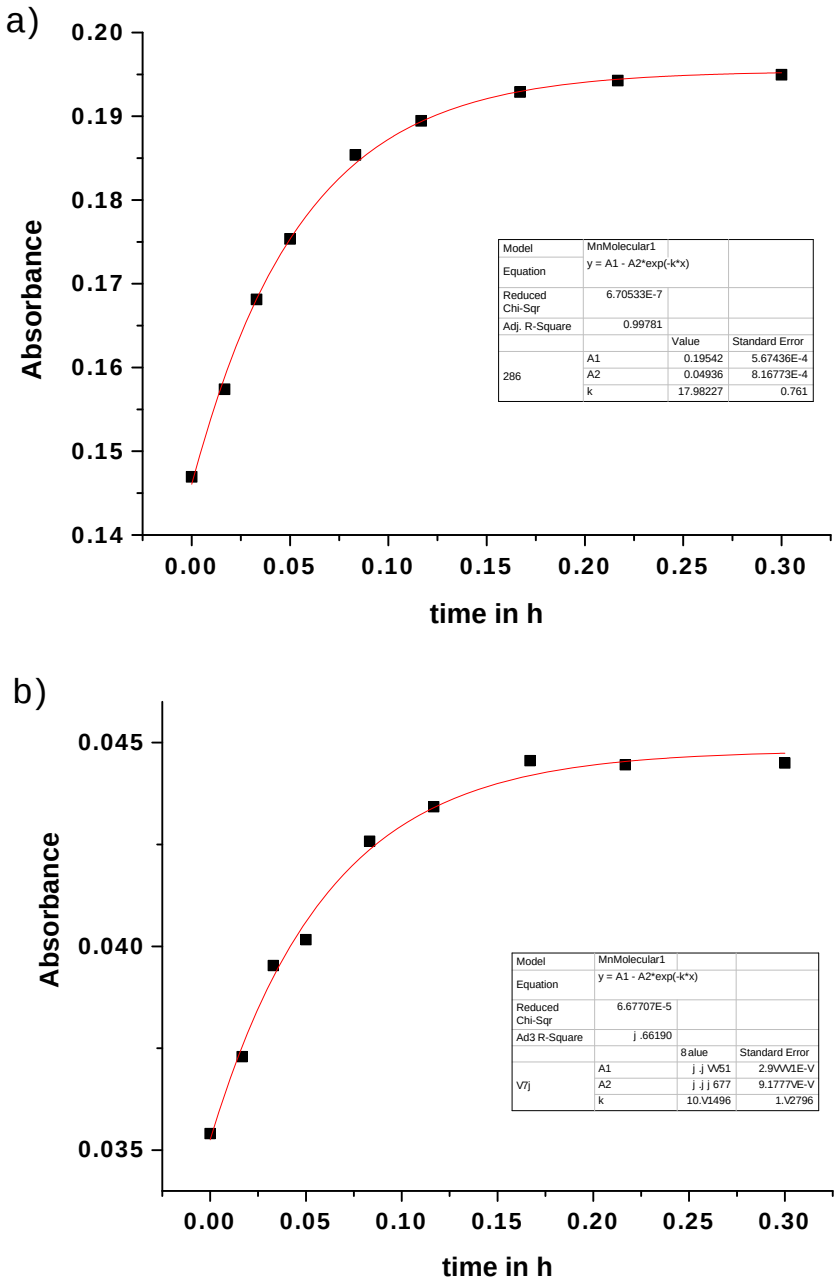

ESI-Figure 3: Monoexponential fits to the absorbance of a 4 µM solution of BTA **1** at 450 nm (a)) and 286 nm (b)) with respect to the UV light irradiation time.

High concentration UV/VIS experiments:

To obtain NMR and UV/Vis spectra at the same sample concentration 1 mg of BTA **1** was dissolved in 0.74 mL DMSO-d_6 (c = 1.8 mM) in an amberized NMR tube. After acquisition of a ^{1}H NMR spectrum parts of the solution were taken from the sample by using a syringe with a 10 cm long PTFE tubing and transferred into a 0.01 mm quartz cuvette to measure an UV/Vis spectrum. Afterwards the NMR sample was irradiated with UV light according to the described *in situ* irradiation procedure. After 15 min of irradiation a second NMR spectrum was acquired and

again a small portion of the solution was transferred to the quartz cuvette. This procedure was repeated after 25 min and 45 min of irradiation with UV light.

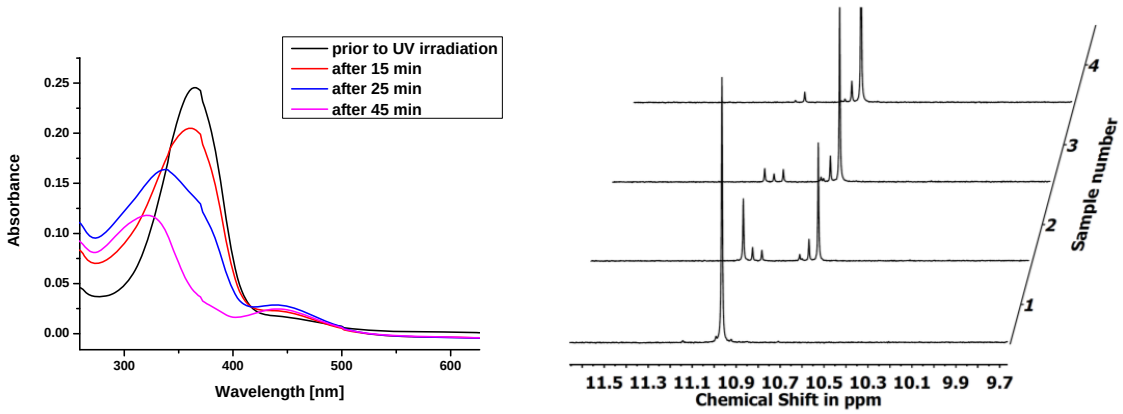

ESI-Figure 4: (left) Absorption spectra of a 1.8 mM sample of BTA **1**, prior to and after irradiation with UV light. (right) ^{1}H NMR spectra (400 MHz, 300 K) of the same sample in DMSO-d_6 acquired prior to the UV Vis spectra. Trace 1: prior to irradiation, trace 2: after 15 min, trace 3: after 25 min and trace 4: after 45 min irradiation with UV light.

Supramolecular stacking of BTAs via H-bonds and π-π-interaction is well known for the BTA **1** in aqueous DMSO and THF.[2] Therefore, we used DMSO-d_6 from an ampulla. Furthermore, NMR spectra of BTA solutions in DMSO-d_6 with different concentration (1.8 mM and 0.18 mM) were measured (ESI-Fig. 5). For these two samples, no differences in chemical shifts can be observed, and an influence of aggregation on the chemical shift can be excluded.

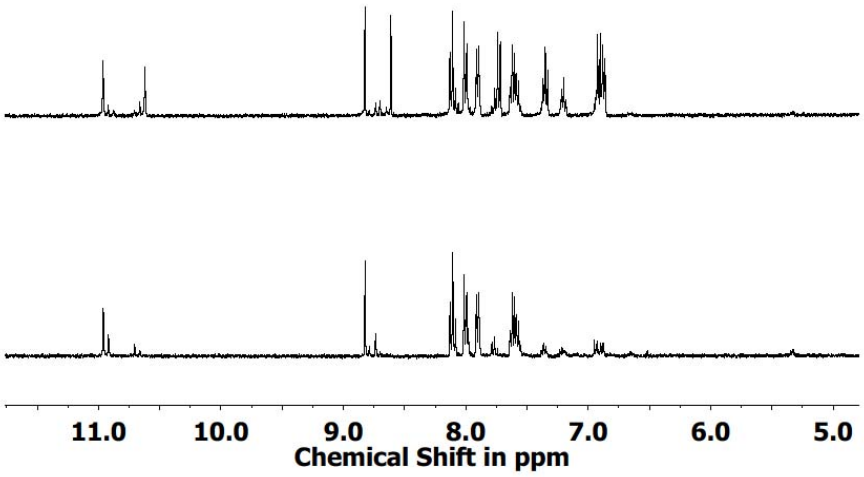

ESI-Figure 5: Upper trace: ^{1}H-NMR spectrum (400 MHz, 300 K) of the 1.8 mM BTA **1** solution in DMSO-d_6, acquired with 16 scans. Lower trace: ^{1}H-NMR spectrum (400 MHz, 300 K) of the 0.18 mM BTA solution in DMSO-d_6, acquired with 512 scans.

ESI-3 NMR experiments

All NMR experiments were performed on a Bruker Avance III HD spectrometer with 700.3 MHz proton frequency, equipped with a 5 mm QCI (^{1}H, ^{13}C, ^{19}F, ^{15}N) CryoProbe with z-gradients, or a Bruker Avance III spectrometer with 600.3 MHz proton frequency, equipped with a 5 mm Triple Resonance Broadband Probe (TBI) (^{1}H, ^{13}C, BB) with z-gradients. NMR samples were prepared in 5 mm amberized tubes (Wilmad LabGlass, 527-PP-7AMB). DMSO-d_6 (99.8 Atom % D) was purchased from Sigma Aldrich in ampulla (0.5 mL or 0.75 mL). All measurements were performed in DMSO-d_6 at 300 K without spinning the sample. Processing of NMR data was applied with Bruker Topspin (Version 3.2 pl3).

For 1D proton spectra FIDs with 24k complex data were sampled within 1 s (600.3 MHz) or 64 k complex data points within 2.3 s (700.3 MHz) over a sweep width of 20 ppm. Prior to Fourier transformation FIDs were zero filled to 64k data points and apodized with an exponential function (LB = 0.3 Hz). Resulting spectra were manually phase corrected and automatically baseline corrected. Series of proton spectra were obtained as pseudo-2D experiments. Acquisition settings for pseudo-2D experiments were chosen comparable to 1D proton experiments. Between single ^{1}H experiments in the pseudo-2D experiments a delay between 2 and 4 minutes was used. All ^{1}H experiments were executed with a single scan. For processing of pseudo-2D data planes, a macro was used, which saved single rows of the data plane into new 1D data sets and automatically applied phase and baseline correction to this 1D datasets. Series of 1D data were integrated with the Bruker macro “intser” and integral values were saved as ASCII files.

ASAP-HSQC experiments were acquired by using the pulse sequence and pulse shapes proposed in the literature, as downloaded from http://www.ioc.kit.edu/luy/110.php (“ASAP-HSQC”).[3] Between consecutive increments in the indirect dimension, an isotopic mixing with a length of 30 ms (DIPSI-2[4]) and a relaxation delay of 150 ms was applied. Acquisition of FIDs was carried out with 1498 data points within 89.88 ms, in echo-antiecho mode, over a spectral width of 9 ppm in the direct dimension and 2k increments over a spectral width of 40 ppm in the indirect dimension, with a single scan per increment. Delays were optimized for a C-H coupling constant of 145 Hz. Resulting FIDs were zero filled to 16k data points in the direct dimension and apodized with squared sine functions (SSB = 2) in both dimensions. Spectra obtained after Fourier transformation of the data planes were manually phase corrected and automatically baseline corrected.

Pure shift BIRD decoupled HSQC spectra were acquired using the pulse sequence proposed in the literature, as downloaded from http://nmr.chemistry.manchester.ac.uk (“pushhsqcrtbird”, version for Bruker instruments).[5] The acquisition of the full length FIDs of 0.18 s in the proton dimension (756 complex data points, dwell time: 238 µs, 6 ppm spectral width) was interrupted five times per FID for insertion of a BIRD decoupling element (half data chunk length “*at/2n*”: 15.2 ms). In the direct dimension 512 increments were collected using a spectral width of 90 ppm. Transmitters were placed at 8 ppm (^{1}H) and 130 ppm (^{13}C). 64 dummy scans and 16 scans per increment were used. A relaxation delay of 4 s was used in-between individual scans. Hard 90°-pulses of 6.7 µs length were used for ^{1}H and of 9.25 µs for ^{13}C. INEPT and BIRD delays were optimized for a one-bond coupling of 145 Hz. During acquisition heteronuclear decoupling was achieved with adiabatic bi-level decoupling[6]. All gradients were of 900 ms length and used a smoothed square shape (SMSQ10.100). Maximum gradient amplitudes used are G_1 = 11%, G_2 = 80%, G_3 = 15% and G_4 = 20.1% of the maximum gradient strength of 53.5 G/cm (for gradient numbering, see [5]). Resulting FIDs were zero filled to 8k data points in the direct dimension and 2k data points in the indirect dimension. Linear forward prediction of complex data was applied for both dimensions using 1k data points for the direct and 512 data points for the indirect dimension. FIDs were apodized with squared sine functions (SSB = 2) in both dimensions. Spectra obtained after Fourier transformation of the data planes were manually phase corrected and automatically baseline corrected.

All other NMR experiments were acquired with pulse sequences from the Bruker pulse sequence library.
HMBC (hmbcgpndqf) experiments were acquired with 2k data points, in QF mode, within 0.84 s over a spectral width of 7 ppm (offset 9 ppm) in the direct dimension and with 256 increments over a spectral width of 90 ppm in the indirect dimension, with four scans per increment. Consecutive scans were started with a relaxation delay of 1.5 s, and coupling evolution period was optimized for a C-H coupling constant of 8 Hz. Prior to Fourier transformation, FIDs were zero filled to 16k data points in the direct dimension and 1k data points in the indirect dimension. Further FIDs were apodized with sine functions (SSB = 0) in both dimensions. Processing was applied in magnitude mode and resulting spectra were automatically baseline corrected.
EASY-ROESY (roesyadjsphpr[7]) experiments were acquired with 2k data points (States-TPPI) in the direct and 1k increments in the indirect dimension with a spectral width of 20 ppm in both dimensions. For each increment 8 consecutive scans with a relaxation delay of 2 s were acquired. A spin lock tilt angle of 45° was applied during the low- and a high field spin lock. Both spin lock blocks are composed of a shaped pulse (ascending half Gaussian pulse), which draws magnetization to the desired spin lock angle, the spin lock pulses to keep the magnetization at this angle and a shaped pulse (descending half Gaussian pulse) to return magnetization into the z-direction. All ramps where applied with a length of 1 ms. With two 100 ms spin locks at constant amplitude, the total spin lock duration amounted to 200 ms plus the duration of the ramps. FIDs were zero-filled to 4k data points in the direct dimension and apodized with squared sine functions (SSB = 2) in both dimensions. After Fourier transformation spectra were manually phase corrected and automatically baseline corrected.
^{1}H-^{15}N-HSQC (hsqcetf3gp) experiments were recorded with 2k data points (Echo-Antiecho) within 0.07 s and a spectral width of 20 ppm in the direct dimension and 512 increments and a spectral width of 32 ppm (Offset: 130 ppm compared to liquid NH_3) in the indirect dimension. For each increment 32 consecutive scans with a relaxation delay of 1 s were accumulated and transfer delays were optimized for an N-H coupling constant of 90 Hz. Prior to Fourier transformation, FIDs were zero filled to 8k data points in the direct dimension. Further FIDs were apodized with squared sine functions (SSB = 2) in both dimensions. After Fourier transformation spectra were manually phase corrected and automatically baseline corrected.

ESI-4 *In situ* irradiation of NMR samples

According to literature, a waveguide (BFH 48-1000, Thorlabs) was inserted within a coaxial stem insert (WGS-5BL-SP – Wilmad LabGlass) into the solution.[8] For UV light irradiation a Nichia SMD LED UV NCSU275 was used. This LED was supplied with a constant current of 500 mA (Lumitronix constant current source). The current applied to the LED was controlled with a relay (Thinkerforge Industrial Quad Relay Bricklet) which is connected to the spectrometer computer via USB. During irradiation with the LED, the applied current as well as voltage are monitored by a Thinkerforge Voltage/Current Bricklet.

Irradiation power was measured with an integration sphere (AVASPHERE-50-IRRAD) and an avaspec UV/VIS detector (AVASPEC-ULS3648*)*. An irradiation power of 0.65 mW/cm² was measured at the roughened waveguide tip prior to NMR measurements.

ESI-5 Chemical shift assignment for the four photoisomers

Chemical shift assignment for the four photoisomers was done in three steps. ^{1}H chemical shifts of the ***ttt*** isomer were obtained from ^{1}H NMR spectra in thermal equilibrium. H_{11} and NH protons can be assigned by relative signal intensity, multiplicity and chemical shift region. All other aromatic protons of the azobenzene moiety can be assigned by analysis of relative signal intensity and information from $^{3}J_{HH}$ coupling constants. For the assignment of H_6 and H_7 an additional EASY-ROESY[7] spectrum was acquired (see ESI-Fig. 6).

ESI-Table 2: ^{1}H chemical shifts, integrals and multiplicity of highly populated species (***ttt***) in the BTA sample in DMSO-d_6 at 300 K prior to UV light irradiation:

^{1}H chemical shift [ppm]	rel. integral	multiplicity	$^{3}J_{HH}$ [Hz]	assignment
10.96	1	s		NH
8.83	1	s		11
8.09	2	d	9.2	7
8.0	2	d	9.2	6
7.9	2	d	7.7	3
7.62	2	pt	7.7	2
7.57	1	pt	-	1

Proton assignment for the ***ccc*** isomer was done similar to the ***ttt*** isomer, but in a PSS upon irradiation with UV light (λ = 365 nm) instead of in thermal equilibrium. Chemical shifts, multiplicity and coupling constants for the ***ccc*** isomer are given in Table 3.

ESI-Table 3: ^{1}H chemical shifts, integrals and multiplicity of highly populated species (***ccc***) in the BTA sample in DMSO-d_6 at 300 K in a PSS upon irradiation with UV light (λ = 365 nm):

^{1}H chemical shift [ppm]	rel. integral	multiplicity	$^{3}J_{HH}$ [Hz]	assignment
10.61	1	s		NH
8.61	1	s		11
7.73	2	d	8.7	7
7.35	2	pt	8	2
7.2	1	pt		1
6.92	2	d	8.7	6
6.87	2	d	8	3

Assignment for the ***ttc*** and the ***tcc*** isomers was achieved by taking the irradiation time into account (thereby estimating the fraction of *trans* and *cis* moieties), so that signals can be assigned to a photoisomer by their intensity in relation to the H_{11} and NH protons (for which it is known to which isomer they belong). Chemical shifts, multiplicity and coupling constants for the ***ttc*** and ***tcc*** isomer are given in Table 4.

ESI-Table 4: ^{1}H chemical shifts, relative integrals and multiplicity of both mixed isomers in the BTA sample in DMSO-d_6 at 300 K during irradiation with UV light (λ = 365 nm):

^{1}H chemical shift [ppm]	rel. integral	multiplicity	$^{3}J_{HH}$ [Hz]	assignment
1st mixed isomer (*ttc*)				
10.91	2	s		NH-trans
10.7	1	s		NH-cis
8.79	1	pt		11 (trans/trans)
8.74	2	d		11 (trans/cis)
8.07	4	d		7-trans
7.99	4	d		6-trans
7.85	4	d		3-trans
7.77	2	d		7-cis
7.62	4	m		2-trans
7.57	4	m		1-trans
7.35	2	m		2-cis
7.2	1	m		1-cis
6.94	2	m		6-cis
6.88	2	m		3-cis
^{1}H chemical shift [ppm]	rel. integral	multiplicity	$^{3}J_{HH}$ [Hz]	assignment
2nd mixed isomer (*tcc*)				
10.87	1	s		NH-trans
10.67	2	s		NH-cis
8.69	2	d		11 (trans/cis)
8.65	1	pt		11 (cis/cis)
8.05	2	d		7-trans
7.97	2	d		6-trans
7.8	2	d		3-trans
7.75	4	d		7-cis
7.62	2	m		2-trans
7.57	1	m		1-trans
7.35	4	m		2-cis
7.2	2	m		1-cis
6.93	4	d		6-cis
6.88	4	d		3-cis

Assignment of the signals of H_7 and H_6 as well as assignment of signals to certain isomers were verified by using an EASY-ROESY experiment.[7] Cross peaks with inverse signal phase relative to the diagonal indicate spatial proximity of two protons, and thereby $H_{7\text{-trans}}$ and $H_{7\text{-cis}}$ can be distinguished from H_6 protons.

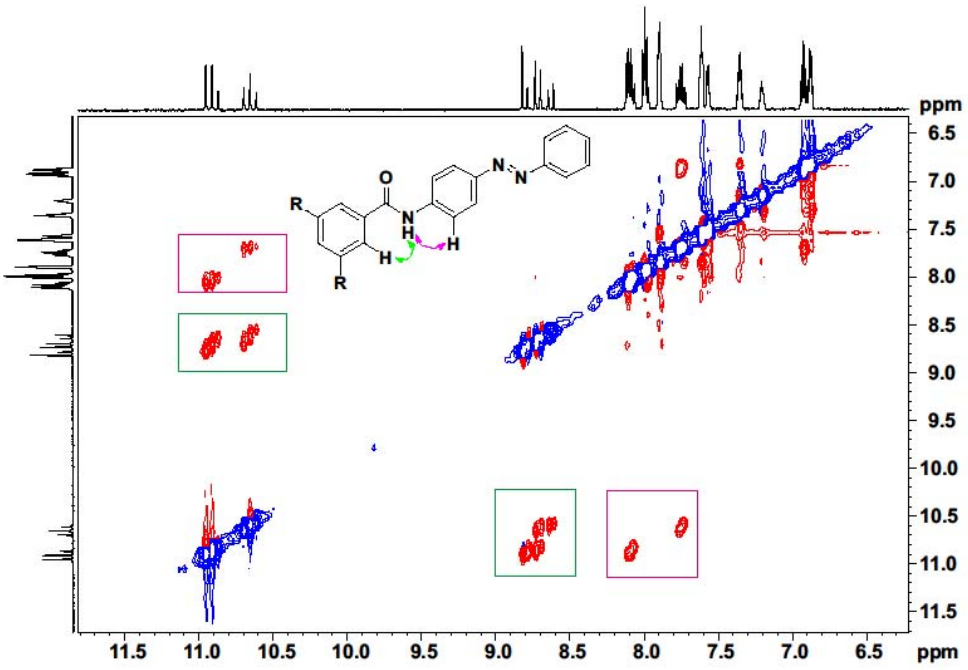

ESI-Figure 6: EASY-ROESY[7] spectrum (700 MHz) of a mixture of all four photoisomers in DMSO-d_6 at 300 K.

HSQC experiments are used to assign carbon atoms in different isomers. In case of a high resolution ASAP-HSQC[3] all C_{11} carbons can be assigned for all four photoisomers by extracting the carbon chemical shift from H_{11}-C_{11} correlations in the ASAP spectrum (ESI-Fig. 7). By using a real-time BIRD decoupled HSQC[5] (ESI-Fig. 8) peak separation in the proton dimension can be achieved and carbon chemical shifts of $C_{7\text{-trans}}$, $C_{7\text{-cis}}$ and $C_{6\text{-trans}}$ can be assigned to certain photoisomers. All other carbons, in which the chemical shift differences between the different isomers are smaller than the spectral resolution (in both dimensions), have a “shared” signal in correlation spectra.

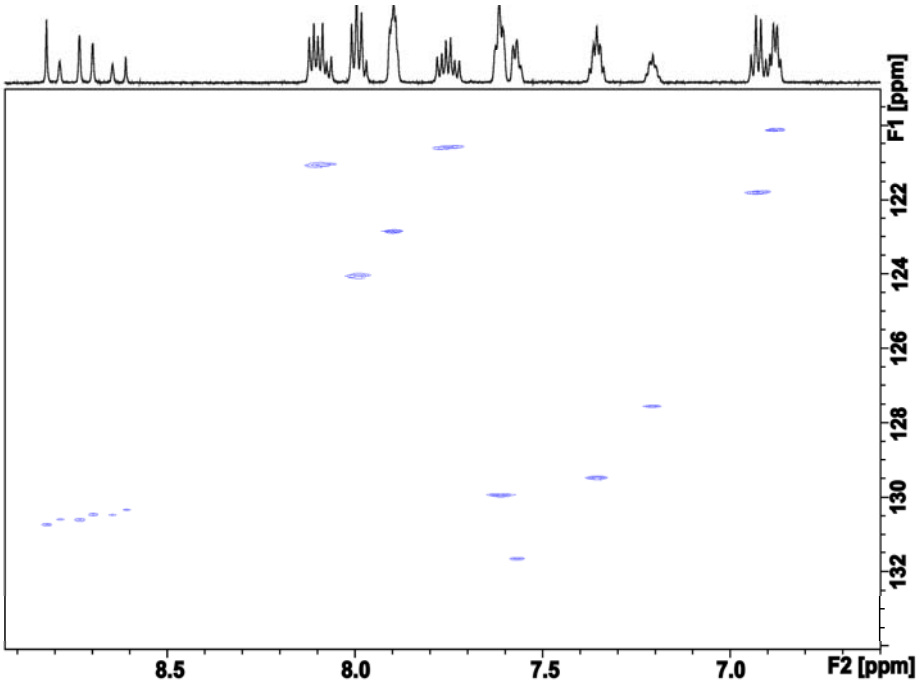

ESI-Figure 7: ASAP-HSQC[3] spectrum (700 MHz) of a mixture of all four photoisomers of the azobenzene benzenetricarboxyamide shown in Fig. 1 of the main article in DMSO-d_6 at 300 K.

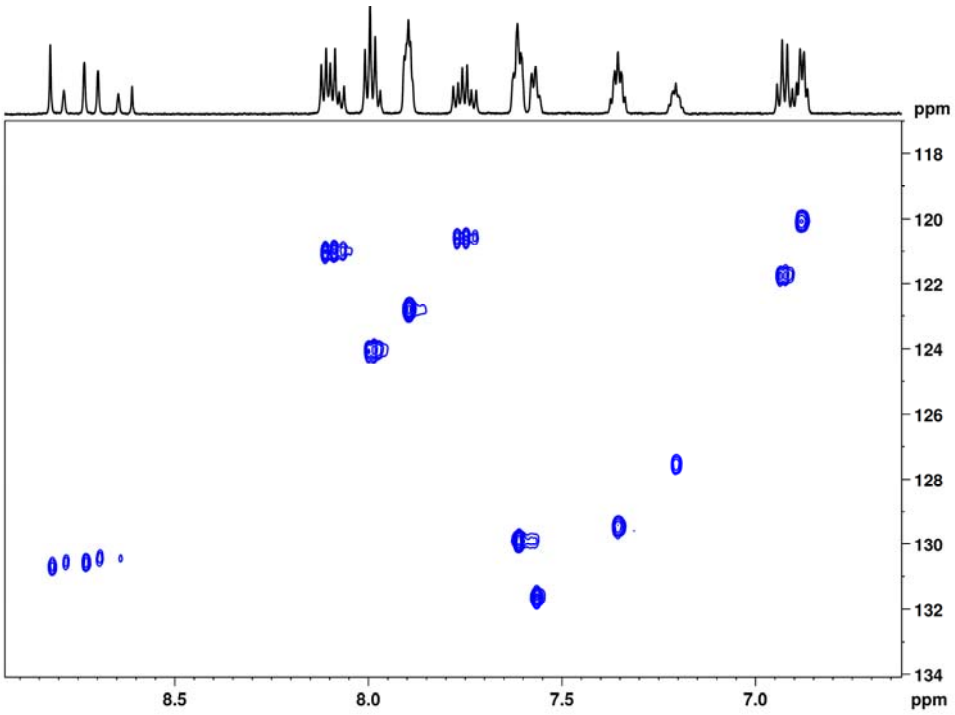

ESI-Figure 8: Real-time BIRD decoupled HSQC[5] of a mixture of all four photoisomers in DMSO-d_6 at 300 K. Instead a projection of the real-time BIRD decoupled HSQC a ^{1}H NMR spectrum recorded at 700 MHz is plotted along F2.

Assignment of quaternary carbons to the respective photoisomers was achieved with a ^{1}H-^{13}C-HMBC experiment (ESI-Fig. 9). For the carbonyl-carbons C_9, chemical shifts are sufficiently different to give rise to separated correlation peaks with the H_{11} protons in the HMBC spectrum, so that assignment of C_9 shifts to certain isomers and sidechains is possible. Correlation peaks from NH protons to the quaternary carbon C_8 are well resolved, too. As a result, assignment of C_8 shifts to the respective isomers and sidechain configurations is feasible.

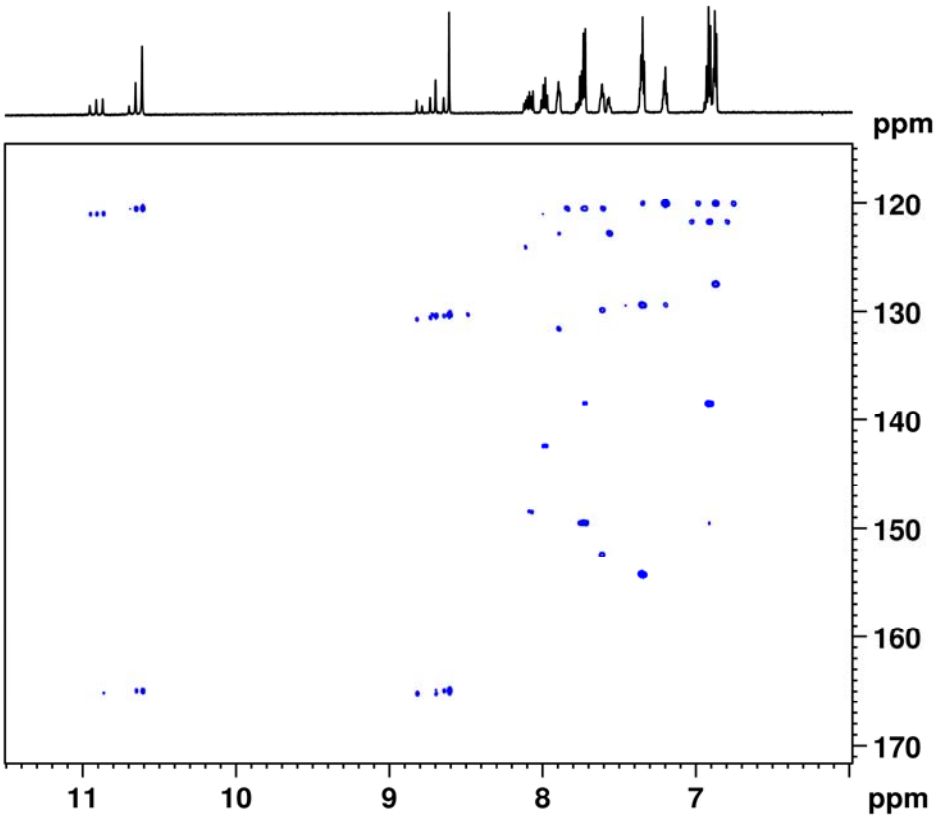

ESI-Figure 9: ^{1}H-^{13}C-HMBC spectrum (700 MHz) of a mixture of all four photoisomers in DMSO-d_6 at 300 K.

The patterns of NH and H_{11} protons of the different photoisomers are quite similar, so that a definite assignment of those ^{1}H resonances can be done by HSQC experiments: NH protons give rise to correlations in a ^{1}H-^{15}N-HSQC and H_{11} protons in a ^{1}H-^{13}C experiment (ESI-Fig. 10).

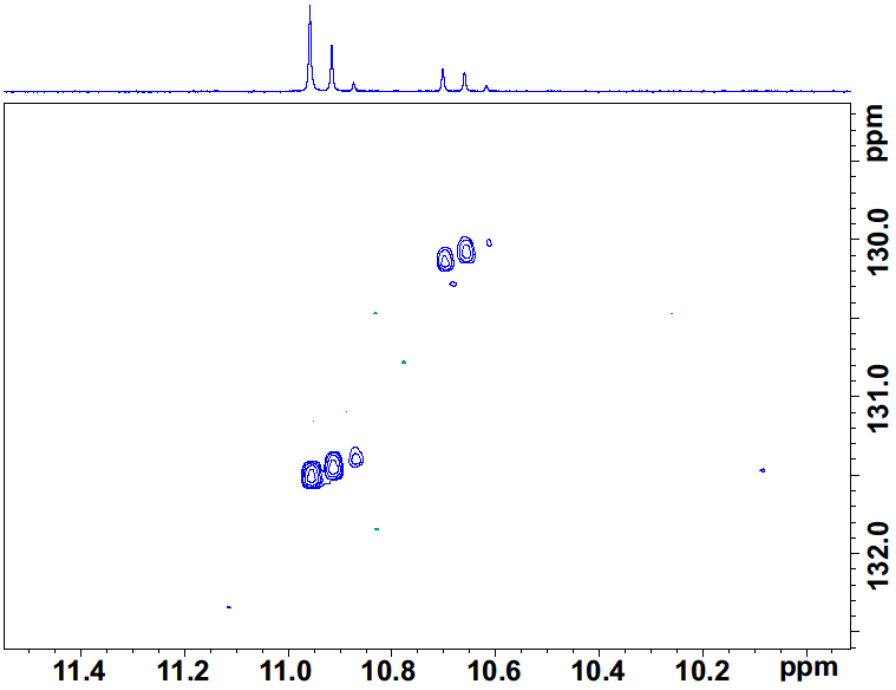

ESI-Figure 10: ^{1}H-^{15}N-HSQC (700 MHz) of a mixture of all four photoisomers in DMSO-d_6 at 300 K.

To visualise the chemical shift development during the photoisomerisation, chemical shifts (Table 2 to Table 4) are shown at the location in the corresponding photoisomer (ESI-Fig. 11).

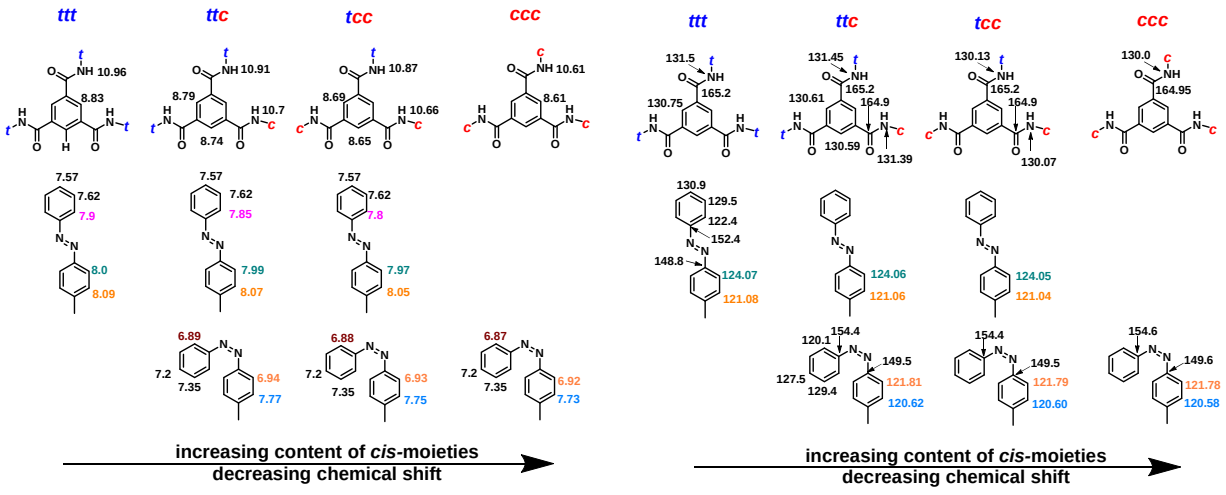

ESI-Figure 11: left: Proton chemical shifts of all four *trans-cis* isomers. Right: Carbon and (amide) nitrogen chemical shifts in the different isomers. For carbon chemical shifts of the *trans* azobenzenes, some chemical shifts are the same in different isomers. Chemical shifts given in black numbers for the *trans* azobenzene in the ***ttt*** isomer are the same for the azobenzenes in the ***ttc*** and ***tcc*** isomers.

ESI-6 Mathematical description of thermal fading

For the azobenzene benzenetricarboxyamide system shown in Fig. 1 of the main article with its four photoisomers ***ttt***, ***ttc***, ***tcc*** and ***ccc*** three consecutive equilibria are considered. It is assumed that the reaction scheme given below describes the interconversion of the configurational isomers under thermal fading and that decomposition reactions can be neglected.

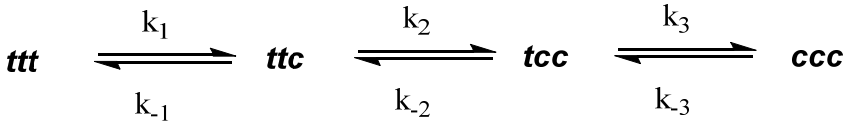

Changes in the concentration are described by following four differential equations.

$$\frac{d}{dt}c_{ttt} = -k_1 c_{ttt} + k_{-1} c_{ttc}$$

$$\frac{d}{dt}c_{ttc} = +k_1 c_{ttt} - (k_{-1} + k_2) c_{ttc} + k_{-2} c_{tcc}$$

$$\frac{d}{dt}c_{tcc} = +k_2 c_{ttc} - (k_{-2} + k_3) c_{tcc} + k_{-3} c_{ccc}$$

$$\frac{d}{dt}c_{ccc} = +k_3 c_{tcc} - k_{-3} c_{ccc}$$

These can be represented in matrix form

$$\frac{d}{dt}\vec{c} = \mathbf{K}\vec{c},$$

where the matrix elements of $\mathbf{K}$ represent the reaction rate constants of the three equilibrium reactions

$$\mathbf{K} = \begin{pmatrix} -k_1 & +k_{-1} & 0 & 0 \\ +k_1 & -(k_{-1} + k_2) & +k_{-2} & 0 \\ 0 & +k_2 & -(k_{-2} + k_3) & +k_{-3} \\ 0 & 0 & +k_3 & -k_{-3} \end{pmatrix}.$$

In addition, vector $\vec{c}$ represents the concentrations *c* of the four photoisomers:

$$\vec{c} = \begin{pmatrix} c_{ttt} \\ c_{ttc} \\ c_{tcc} \\ c_{ccc} \end{pmatrix}$$

Similarly, when expressing the rate laws in terms of molar fractions *X*, we find

$$\frac{d}{dt}\vec{X} = \mathbf{K}\vec{X}, \text{with } \vec{X} = \begin{pmatrix} X_{ttt} \\ X_{ttc} \\ X_{tcc} \\ X_{ccc} \end{pmatrix}.$$

Integration is performed iteratively during the fitting process, starting from a set of initial molar fractions $X_{i,0}$ using

$$\vec{X}(t + \Delta t) = \vec{X}(t) + \left(\mathbf{K} \times \vec{X}(t)\right) * \Delta t,$$

with the time step chosen being much smaller than the biggest component of $\mathbf{K}$. For an alternative approach, closed analytical solution for such a reaction scheme can be found in [9].

$$|\Delta t| \leq \left(32 * \max\left(\left|K_{ij}\right|\right)\right)^{-1}$$

For fitting, a good initial guess was obtained by reading the initial molar fractions $X_{i,0}$ from the data and fixing t_0 (t_0 was not a variable during the fitting). For the rate constants quite arbitrary initial guesses were used. The fitting routine constrained all initial molar fractions to $0 < X_{i,0} < 1$ and all rate constants to $k_i > 0$. The fitting routine was implemented as user-defined fitting function into IGOR Pro 6.3 © WaveMetrics, Inc., which reports fitting errors only representing statistical uncertainty of the coefficient values (assuming the data to be described well by the model and the data to be normally distributed around the fitting function). Direct comparison between the rate constants using the signals for the amide signals (NH) and the signals of the aromatic protons H_{11} illustrates, that error estimates from the fitting routine largely underestimate the minimum error ranges that actually need to be assumed for the rate constants reported (see ESI-Table 5). Thus an estimate for the minimum uncertainty of the rate constants is ($k_{-x} \approx \pm 0.03$ day^{-1}).

ESI-Table 5: Reaction rate constants from the fitting procedure for conversion curves obtained from the NH signals (ESI-Fig. 12) and curves calculated from H_{11} signal integrals (ESI-Fig. 13). The error ranges indicated are reported as obtained from the fitting routine.

k [days^{-1}]	NH	H_{11}
k_1	0.0477 ± 0.0005	0.0327 ± 0.0005
k_{-1}	0.5090 ± 0.0005	0.4778 ± 0.0005
k_2	0.0321 ± 0.0005	0.0253 ± 0.0005
k_{-2}	0.9784 ± 0.0008	0.9703 ± 0.0007
k_3	0.0339 ± 0.0006	0.0088 ± 0.0008
k_{-3}	1.4863 ± 0.0017	1.4654 ± 0.0011

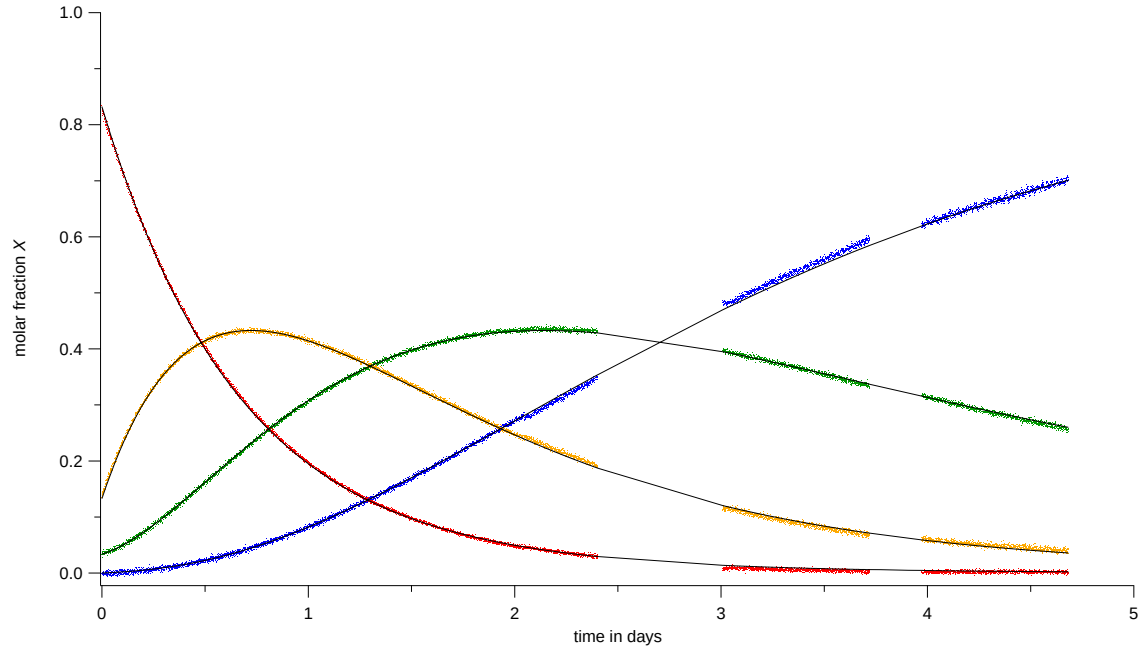

ESI-Figure 12: Thermal fading calculated from integrals of the NH signals of all four photoisomers (not shown in the main text) and fitting results. X_{ttt} is shown in blue, X_{ttc} is shown in green, X_{tcc} is shown in yellow and X_{ccc} is shown in red. The fit to all four curves is shown as black lines.

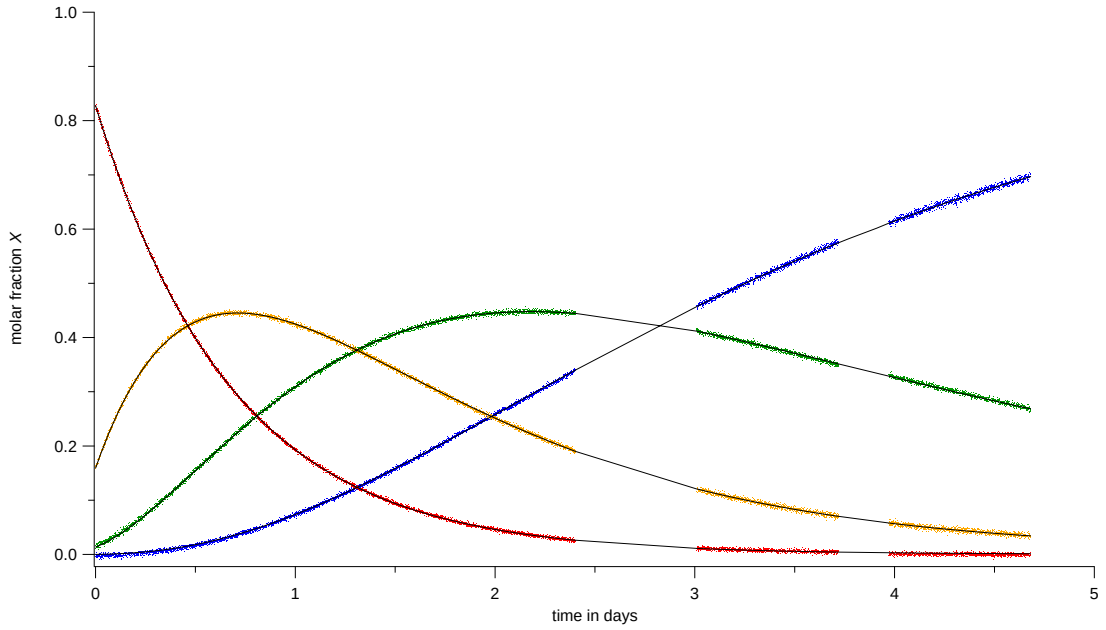

ESI-Figure 13: Thermal fading calculated from integrals of the H_{11} signals of all four photoisomers (equivalent to Fig. 6 in the main text) and results of the fitting procedure. Same colour coding used as in ESI-Fig. 12.

ESI-7 Calculation of equilibrium fractions of all photoisomers from the reaction rate constants

From the set of differential equations listed above (assuming their validity), the relation between the equilibrium concentrations (c_{eq}) and the rate constants *k* obtained can be derived. In the stationary state we obtain:

$$\frac{d}{dt}c_{ttt}\Big|_{t\to\infty} = -k_1 c_{ttt,eq} + k_{-1} c_{ttc,eq} = 0$$

$$c_{ttt,eq} = c_{ttc,eq}\frac{k_{-1}}{k_1}$$

$$\frac{d}{dt}c_{ttc}\Big|_{t\to\infty} = k_1 c_{ttc,eq}\frac{k_{-1}}{k_1} - (k_{-1}+k_2)c_{ttc,eq} + k_{-2}c_{tcc,eq} = 0$$

$$c_{ttc,eq} = c_{tcc,eq}\frac{k_{-2}}{k_2}$$

$$\frac{d}{dt}c_{tcc}\Big|_{t\to\infty} = k_2 c_{tcc,eq}\frac{k_{-2}}{k_2} - (k_{-2}+k_3)c_{tcc,eq} + k_{-3}c_{ccc,eq} = 0$$

$$c_{tcc,eq} = c_{ccc,eq}\frac{k_{-3}}{k_3}$$

Mass balances requires that

$$c_{ttt,eq} + c_{ttc,eq} + c_{tcc,eq} + c_{ccc,eq} = c_{total}\,,$$

which, after inserting the equilibrium ratios shown above, yields:

$$c_{ttt,eq} = \frac{c_{total}}{\left[\left(\frac{k_3}{k_{-3}} + 1\right)\frac{k_2}{k_{-2}} + 1\right]\frac{k_1}{k_{-1}} + 1}$$

$$c_{ttc,eq} = \frac{c_{total}}{\left(\frac{k_3}{k_{-3}} + 1\right)\frac{k_2}{k_{-2}} + 1 + \frac{k_{-1}}{k_1}}$$

$$c_{tcc,eq} = \frac{c_{total}}{\left(\frac{k_{-1}}{k_1} + 1\right)\frac{k_{-2}}{k_2} + 1 + \frac{k_3}{k_{-3}}}$$

$$c_{ccc,eq} = \frac{c_{total}}{\left[\left(\frac{k_{-1}}{k_1} + 1\right)\frac{k_{-2}}{k_2} + 1\right]\frac{k_{-3}}{k_3} + 1}$$

Equilibrium molar fractions are obtained using $X_i = c_i / \sum c_i$:

$$X_{ttt,eq} = \frac{1}{\left[\left(\frac{k_3}{k_{-3}} + 1\right)\frac{k_2}{k_{-2}} + 1\right]\frac{k_1}{k_{-1}} + 1}$$

$$X_{ttc,eq} = \frac{1}{\left(\frac{k_3}{k_{-3}} + 1\right)\frac{k_2}{k_{-2}} + 1 + \frac{k_{-1}}{k_1}}$$

$$X_{tcc,eq} = \frac{1}{\left(\frac{k_{-1}}{k_1} + 1\right)\frac{k_{-2}}{k_2} + 1 + \frac{k_3}{k_{-3}}}$$

$$X_{ccc,eq} = \frac{1}{\left[\left(\frac{k_{-1}}{k_1} + 1\right)\frac{k_{-2}}{k_2} + 1\right]\frac{k_{-3}}{k_3} + 1}$$

From the ratios of rate constants given above, it is now possible to extrapolate to the equilibrium molar fractions using the equations given in the section “ESI-6 Mathematical descriptions of thermal fading”. The values obtained are listed here for both the results obtained from fitting the molar fractions calculated from the NH and the H_{11} integrals:

ESI-Table 6: Equilibrium fractions of all four photoisomers calculated from rate constants obtained fitting from NH and H_{11} and from integration of H_{11} in ^{1}H NMR spectrum prior to irradiation:

Isomer	X_{eq} Fitting NH	X_{eq} Fitting H_{11}	X_{eq} Integration H_{11}
ttt	**0.9117**	**0.9343**	**~0.93**
ttc	**0.0854**	**0.0640**	**~0.07**
tcc	**0.0028**	**0.0017**	
ccc	**6.4e-5**	**1.0e-5**	

ESI-8 Photoreaction with visible light

A deviation from the rate laws used to describe thermal relaxation was observed for an induced relaxation of the sample by irradiation with visible light (λ = 447 nm). In this case, an exponential decay of the ***ccc*** fraction is observed, but only the ***tcc*** fraction undergoes a maximum of about 40 %. Fractions of the ***ttc*** and ***ttt*** show an exponential growth. In contrast to the thermal equilibrium, irradiation with blue light leads to another PSS in which three photoisomers are populated (20 % ***tcc***, 40 % ***ttc*** and 40 % ***ttt***).

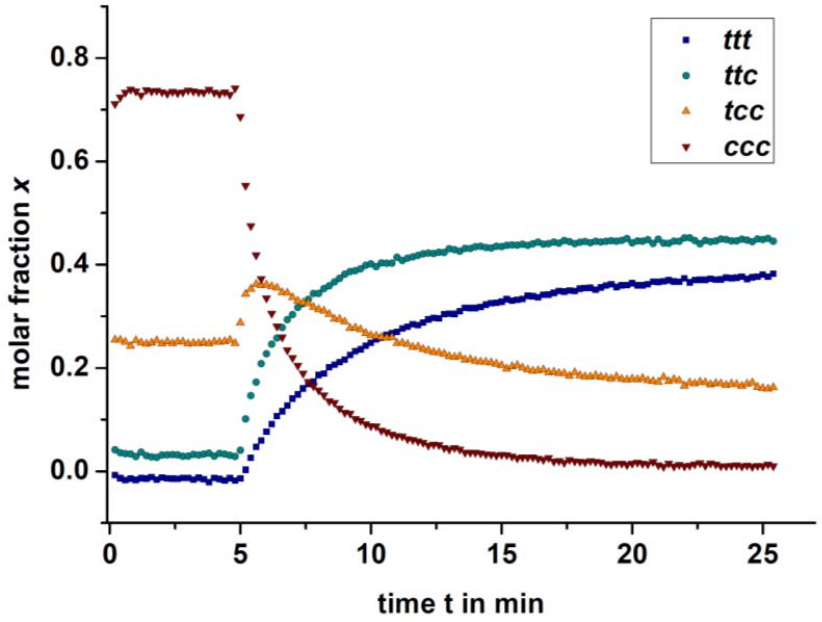

ESI-Figure 14: Induced Relaxation from PSS (UV) to another PSS (blue light, λ = 447 nm). Fraction calculated from integrals of H_{11} of the four different photoisomers. ^{1}H-NMR spectra (600 MHz) were measured in DMSO-d_6 at 300 K.

ESI-9 Literature

1. L. M. Goldenberg, L. Kulikovsky, O. Kulikovska, J. Tomczyk and J. Stumpe, *Langmuir*, 2010, **26**, 2214-2217.
2. S. Lee, S. Oh, J. Lee, Y. Malpani, Y.-S. Jung, B. Kang, J. Y. Lee, K. Ozasa, T. Isoshima, S. Y. Lee, M. Hara, D. Hashizume and J.-M. Kim, *Langmuir*, 2013, **29**, 5869-5877.
3. D. Schulze-Sünninghausen, J. Becker and B. Luy, *J. Am. Chem. Soc.*, 2014, **136**, 1242-1245.
4. S. P. Rucker and A. J. Shaka, *Mol. Phys.*, 1989, **68**, 509-517.
5. L. Paudel, R. W. Adams, P. Király, J. A. Aguilar, M. Foroozandeh, M. J. Cliff, M. Nilsson, P. Sándor, J. P. Waltho and G. A. Morris, *Angew. Chem. Int. Ed.*, 2013, **52**, 11616-11619.
6. Ē. Kupce, R. Freeman, G. Wider and K. Wüthrich, *J. Mag. Reson.*, 1996, **122**, 81-84.
7. C. M. Thiele, K. Petzold and J. Schleucher, *Chem. Eur. J.*, 2009, **15**, 585-588.
8. C. Feldmeier, H. Bartling, K. Magerl and R. M. Gschwind, *Angew. Chem. Int. Ed.*, 2015, **54**, 1347-1351.
9. H. Mauser and G. Gauglitz, eds., *Photokinetics: Theoretical Fundamentals and Applications*, Elsevier Science, Amsterdam, 1998.